Synthesis and Characterization of Rhodium Complexes Containing 2,4,6-Tris(2-pyridyl)-1,3,5-triazine and Its Metal-Promoted Hydrolytic Products: Potential Uses of the New Complexes in Electrocatalytic Reduction of Carbon Dioxide

Parimal Paul,*,† Beena Tyagi,† Anvarhusen K. Bilakhiya,† Mohan M. Bhadbhade,‡ Eringathodi Suresh,‡ and G. Ramachandraiah§

Disciplines of Silicates and Catalysis, Sophisticated Analytical Instruments Laboratory, and Discipline of Reactive Polymers, Central Salt and Marine Chemicals Research Institute, Bhavnagar 364 002, India

Received August 1, 1997

The reaction of 2,4,6-tris(2-pyridyl)-1,3,5-triazine (tptz) with $RhCl_3 \cdot 3H_2O$ has been studied under different experimental conditions. This reaction in ethanol resulted in the formation of $[Rh(tptz)Cl_3] \cdot 2H_2O$ (**1**), whereas the bis-chelate complex $[Rh(tptz)_2][ClO_4]_3 \cdot 2H_2O$ (**2**) was obtained in a two-step reaction in acetone; the chlorides from $RhCl_3$ were removed in the first step using $AgClO_4$, and the ligand tptz was added in the second step. Complexes **1** and **2**, when refluxed in ethanol−water (1:1), resulted in metal-promoted hydrolysis of tptz to bis-(2-pyridylcarbonyl)amide anion (bpca) and 2-picolinamide (pa), yielding the complexes $[Rh(bpca)(pa)Cl][PF_6] \cdot H_2O$ (**3**) and $[Rh(bpca)_2][ClO_4]$ (**6**), respectively. A mixed-ligand complex, $[Rh(bpca)(tpy)][PF_6]_2 \cdot CH_3CN$ (**4**), was obtained by the reaction of either **1** with tpy or $[Rh(tpy)Cl_3]$ (**5**) with tptz in ethanol−water medium. The crystal structures of complexes **1** and **4** have been determined. Crystal data: complex **1**, monoclinic, $P2_1/c$, $a = 11.642(2)$ Å, $b = 7.302(2)$ Å, $c = 24.332(3)$ Å, $\beta = 96.420(10)°$, $Z = 4$, $R = 0.040$, and wR2 = 0.117; complex **4**, triclinic, $P\bar{1}$, $a = 9.581(1)$ Å, $b = 12.933(2)$ Å, $c = 14.493(2)$ Å, $\alpha = 82.480(10)°$, $\beta = 71.810(10)°$, $\gamma = 75.100(10)°$, $Z = 2$, $R = 0.030$, and wR2 = 0.082. The two water molecules of complex **1** make short contacts with the carbon atoms adjacent to the metal-bound nitrogen atom of the triazine ring; this observation provides some insight about the "intermediate" of the hydrolysis. X-ray and NMR data suggest that the electron-withdrawing effect of the metal ion is the major responsible factor for the hydrolysis of tptz. The cyclic voltammograms of the complexes exhibit a metal-based 2e reduction (Rh(III) → Rh(I)) at the potential range −0.42 to −0.98 V vs SCE, followed by ligand-based redox couple(s). These novel complexes show effective catalytic properties for the electrocatalytic reduction of carbon dioxide in the potential range −1.26 to −1.44 V.

Introduction

The ligand 2,4,6-tris(2-pyridyl)-1,3,5-triazine (tptz) has been used as an analytical reagent for various metal ions.[1−6] A number of transition-metal and lanthanide complexes of the same ligand have also been reported.[7−25]

In recent years, tptz which functions simultaneously as a tridentate and a bidentate ligand, has gained considerable interest because of its use as a spacer for designing supramolecular complexes.[26−30] These complexes can be used in a variety of

* To whom correspondence should be addressed.
† Discipline of Silicates and Catalysis.
‡ Sophisticated Analytical Instruments Laboratory.
§ Discipline of Reactive Polymers.

(1) Collins, P.; Diehl, H.; Smith, G. F. *Anal. Chem.* **1959**, *31*, 1862.
(2) Collins, P.; Diehl, H. *Anal. Chim. Acta* **1960**, *22*, 125.
(3) Diehl, H.; Buchanan, E. B., Jr.; Smith, G. F. *Anal. Chem.* **1960**, *33*, 1117.
(4) Tsen, C. C. *Anal. Chem.* **1961**, *33*, 849.
(5) Embry, W. A.; Ayres, G. H. *Anal. Chem.* **1968**, *40*, 1499.
(6) Janmohamed, M. J.; Ayres, G. H. *Anal. Chem.* **1972**, *44*, 2263.
(7) Vagg, R. S.; Warrener, R. N.; Watton, E. C. *Aust. J. Chem.* **1969**, *22*, 141.
(8) Goodwin, H. A.; Sylva, R. N.; Vagg, R. S.; Watton, E. C. *Aust. J. Chem.* **1969**, *22*, 1605.
(9) Kingston, J. V.; Krankovits, E. M.; Magee, R. J.; Watton, E. C.; Vagg, R. S. *Inorg. Nucl. Chem. Lett.* **1969**, *5*, 445.
(10) Vagg, R. S.; Warrener, R. N.; Watton, E. C. *Aust. J. Chem.* **1967**, *20*, 1841.
(11) Barclay, G. A.; Vagg, R. S.; Watton, E. C. *Aust. J. Chem.* **1969**, *22*, 643; *Acta Crystallogr., Sect. B.* **1977**, *B13*, 3487.
(12) Barclay, G. A.; Vagg, R. S.; Watton, E. C. *Acta Crystallogr., Sect. B* **1978**, *B34*, 1833.
(13) Pagenkopf, G. K.; Margerum, D. W. *Inorg. Chem.* **1968**, *7*, 2514.
(14) Fraser, F. H.; Epstein, P.; Macero, D. J. *Inorg. Chem.* **1972**, *11*, 2031.
(15) Durharm, D. A.; Frost, G. H.; Hart, F. A. *J. Inorg. Nucl. Chem.* **1969**, *31*, 571.
(16) Prasad, J.; Peterson, N. C. *Inorg. Chem.* **1971**, *10*, 88.
(17) Taylor, P. J.; Schitt, A. A. *Inorg. Chim. Acta* **1971**, *5*, 691.
(18) Sedney, D.; Kahjehnassiri, M.; Reiff, W. M. *Inorg. Chem.* **1981**, *20*, 3476.
(19) Halfpenny, J.; Small, R. W. H. *Acta Crystallogr.* **1982**, *B38*, 939.
(20) Tokel-Takvoryan, N. E.; Hemingway, R. E.; Bard, A. J. *J. Am. Chem. Soc.* **1973**, *95*, 6582.
(21) Lin, C. T.; Bottcher, W.; Chou, M.; Creutz, C.; Sutin, N. *J. Am. Chem. Soc.* **1976**, *98*, 6536.
(22) Arif, A. M.; Hart, F. A.; Hursthouse, M. B.; Thornton-Pett, M.; Zhu, W. *J. Chem. Soc., Dalton Trans.* **1984**, 2449.
(23) Byers, P.; Chan, G. Y. S.; Drew, M. G. B.; Hudson, M. J.; Madic, C. *Polyhedron* **1996**, *15*, 2845.
(24) Chan, G. Y. S.; Drew, M. G. B.; Hudson, M. J.; Isaacs, N. S.; Byers, P.; Madic, C. *Polyhedron* **1996**, *15*, 3385.
(25) Gelling, A.; Olsen, M. D.; Orrell, K. G.; Osborne, A. G.; Sik, V. *J. Chem. Soc., Chem. Commun*, **1997**, 587.
(26) Thomas, N. C.; Foley, B. L.; Rheingold, A. L. *Inorg. Chem.* **1988**, *27*, 3426.
(27) Chirayil, S.; Hegde, V.; Jahng, Y.; Thummel, R. P. *Inorg. Chem.* **1991**, *30*, 2821.
(28) Gupta, N.; Grover, N.; Neyhart, G. A.; Singh, P.; Thorp, H. H. *Inorg. Chem.* **1993**, *32*, 310.
(29) Berger, R. M.; Holcombe, J. R. *Inorg. Chim. Acta* **1995**, *232*, 217.
(30) Berger, R. M.; Ellis, D. D., II. *Inorg. Chim. Acta* **1996**, *241*, 1.

10.1021/ic9709739 CCC: $15.00
Published on Web 10/07/1998

electrocatalytic/photocatalytic reactions. The compounds of the family 2,4,6-triaryltriazines are usually stable toward hydrolysis; concentrated mineral acid and temperatures above 150 °C are required for their hydrolytic reaction.[31] However, Lerner and Lippard found for the first time that Cu(II) in aqueous media promoted the hydrolysis of tptz to bis(2-pyridylcarbonyl)amide anion;[32,33] crystallographic characterizations of Cu(II) complexes with hydrolyzed tptz were also reported.[34,35]

We were interested in exploring the rhodium chemistry of tptz with a view to prepare mononuclear complexes which can be utilized as building blocks to develop supramolecular systems. Recently we studied the reaction of $RhCl_3$ and $RuCl_3$ with tptz in ethanol−water; $RhCl_3$ promoted the hydrolysis of the ligand to bis(2-pyridylcarbonyl)amide anion (bpca) and afforded the complex $[Rh(bpca)_2]^+$,[36] while $RuCl_3$ under similar reaction conditions yielded a Ru(II) complex with intact tptz, $[Ru(tptz)_2]^{2+}$.[27,36] However, with a judicious choice of solvent and reaction conditions we were able to prepare rhodium complexes of intact tptz. Hydrolysis of tptz in these complexes also occurred on reflux in ethanol−water. This reaction in the presence of 2,2′:6′,2″-terpyridine (tpy) yielded a mixed-ligand complex with one hydrolyzed tptz. Herein we report the synthesis and structural and spectroscopic characterization of a new family of complexes, mechanistic aspects of the hydrolytic reaction, and the potential use of these complexes in the electrocatalytic reduction of carbon dioxide.

Experimental Section

Materials. The ligand 2,4,6-tris(2-pyridyl)-1,3,5-triazine (tptz), 2,2′:6′,2″-terpyridine (tpy), silver perchlorate, ammonium hexafluorophosphate, and tetrabutylammonium tetrafluoroborate were purchased from Aldrich. Hydrated rhodium trichloride was purchased from Arora Matthey. All organic solvents were of reagent grade and were purified by standard methods before use.

Physical Measurements. Conductivity measurements were performed on a Model D1-909 Digisun Electronic digital conductivity meter. Infrared spectra were recorded on a Bio-Rad FTS-40 spectrophotometer as KBr pellets. The UV/vis spectra were recorded on a Model 8452A Hewlett-Packard diode array spectrophotometer. NMR spectra were recorded on a Model DPX 200 Bruker FT-NMR instrument. Cyclic voltammograms were recorded on a EG & G PAR Model 273A potentiostat coupled with a three-electrode cell assembly and Gateway 2000 (4DX2-66) computer equipped with electrochemistry software (Model 270). The three-electrode system consisted of a glassy-carbon working electrode, a platinum-wire auxiliary electrode, and a Ag/AgCl reference electrode. The platinum wire was separated from the analytical solution by a Vycor tip bridge. Solutions of the complexes (1 mM) in purified DMF containing 0.1 M tetrabutylammonium tetrafluoroborate (TBATB) as supporting electrolyte were deaerated by bubbling argon for 20 min prior to each experiment. For experiments under carbon dioxide, the solutions were saturated with CO_2 by bubbling for 30 min.

Controlled-potential electrolysis experiments for the electrocatalytic reduction of carbon dioxide were performed on a EG & G PAR Model 173 galvanostat and 179 digital integrator in a three-compartment cell. The auxiliary Pt mesh and the reference SCE electrodes were separated from the main compartment cell by fine glass frits. In the main compartment, which contained a platinum gauze as working electrode, a 1 mM solution (25 mL) of the complex was taken and purged with carbon dioxide for 30 min prior to electrolysis. However, slow purging of carbon dioxide and stirring of the analytical solution were continued during electrolysis. Electrocatalysis experiments were carried out for 5−6 h at a potential 0.05 V more negative than the respective potentials at which reduction of carbon dioxide occurred.

Product Analysis. Elemental analyses (C, H, and N) were performed on a Model 2400 Perkin-Elmer elemental analyzer. The analysis of formic acid was carried out by following a published procedure[37−39] using chromotropic acid. After electrolysis, 0.5 mL of the reaction mixture was treated with 2 N HCl (0.5 mL) and freshly prepared magnesium powder was added until no more gas evolved. To this solution were added sulfuric acid (12 N, ca. 2 mL) and chromotropic acid (excess), and the reaction mixture was incubated at 60 °C for 30 min, during which time a violet-pink color developed. The volume of the solution was made up to 10 mL, and its absorbance spectrum was recorded; the solution electrolyzed in the absence of carbon dioxide was used as a reference. These spectra exhibit strong bands at 584 (ϵ 950) and 480 nm (ϵ 640), indicating the presence of formic acid; its amount was estimated from a calibration curve made with solutions of known concentrations. The possibility of formation of oxalate was also examined by ^{13}C NMR spectra as follows: after electrolysis the solvent of the reaction mixture was removed by rotary evaporation and the residue was extracted with D_2O (metal complexes are insoluble in water); $^{13}C\{^1H\}$ NMR spectra of the solutions thus obtained were recorded. The spectrum exhibits four large signals at 13.4, 19.7, 23.7, and 58.6 ppm due to Bu_4N^+ (from supporting electrolyte) and two small signals at 165.3 and 166.1 ppm. To compare this spectrum to those of authentic samples, we recorded ^{13}C NMR spectra of the following mixtures of compounds in D_2O under similar conditions. These mixtures are as follows: Bu_4NBF_4 and ammonium oxalate; Bu_4NBF_4, ammonium oxalate, and DMF; Bu_4NBF_4, oxalic acid, and formic acid. The analysis of the data shows that chemical shifts due to Bu_4NBF_4 appear at the same position as mentioned above and resonances due to oxalic acid, DMF, formic acid, and oxalate appear at 162.8, 165.4, 166.2, and 171.6 ppm, respectively. Therefore, the chemical shifts at 165.3 and 166.1 ppm in the D_2O extract of the analytical samples are due to small quantities of DMF and formic acid, indicating no production of oxalate (during evaporation of DMF most of the formic acid, bp 100−101 °C, was evaporated; only small quantities of formic acid and DMF trapped in the solid residue gave small signals). Analysis of gaseous products was not carried out, as slow purging of carbon dioxide was continued during electrolysis.[39]

Synthesis of Metal Complexes. $[Rh(tptz)Cl_3]\cdot 2H_2O$ (1). $RhCl_3\cdot 3H_2O$ (0.263 g, 1 mmol) and tptz (0.312 g, 1 mmol) were taken up in ethanol (40 mL), and the reaction mixture was refluxed for 2 h. The light green microcrystalline compound separated during reflux was isolated by filtration, washed with water, hot ethanol, and diethyl ether, and recrystallized from boiling acetonitrile; yield 0.478 g (85%). Anal. Calcd for $C_{18}H_{16}Cl_3RhN_6O_2$: C, 38.77; H, 2.89; N, 15.07. Found: C, 38.62; H, 2.69; N, 14.94. Molar conductance (Λ_M, Ω^{-1} cm^2 mol^{-1}): 12. ^1H NMR (δ (ppm), DMSO-d_6): 7.93 (m, 1H), 8.35 (m, 3H), 8.67 (t, 2H), 9.07−9.16 (m, 4H), 9.43 (d, 2H). UV/vis (DMF; λ_{max}, nm (ϵ)): 400 (3.5×10^3), 300 (2.4×10^4), 278 (2.1×10^4).

$[Rh(tptz)_2][ClO_4]_3\cdot 2H_2O$ (2). $RhCl_3\cdot 3H_2O$ (0.132 g, 0.5 mmol) and $AgClO_4$ (0.311 g, 1.5 mmol) were taken up in acetone (30 mL), and the reaction mixture was refluxed for 2 h with stirring under an argon atmosphere. The precipitated AgCl was removed by filtration, tptz (0.312 g, 1 mmol) was added to the filtrate, and refluxing was continued for 2 h. The light green microcrystalline compound separated during reflux was isolated by filtration, washed with hot ethanol and diethyl ether, and dried in vacuo; yield 0.36 g (68%). Anal. Calcd for $C_{36}H_{28}Cl_3RhN_{12}O_{14}$: C, 40.72; H, 2.66; N, 15.83. Found: C, 40.81; H, 2.56; N, 15.78. Molar conductance (Λ_M, Ω^{-1} cm^2 mol^{-1}): 210. ^1H NMR

(31) Smolin, E. M.; Rapoport, L. *S-Triazines and Derivatives*; Interscience: New York, 1959; p 163.
(32) Lerner, E. I.; Lippard, S. J. *J. Am. Chem. Soc.* **1976**, *98*, 5397.
(33) Lerner, E. I.; Lippard, S. J. *Inorg. Chem.* **1977**, *16*, 1546.
(34) Cantarero, A.; Amigo, J. M.; Faus, J.; Julve, M.; Debaerdemaeker, T. *J. Chem. Soc., Dalton Trans.* **1988**, 2033.
(35) Faus, J.; Julve, M.; Amigo, J. M.; Debaerdemaeker, T. *J. Chem. Soc., Dalton Trans*. **1989**, 1681.
(36) Paul, P.; Tyagi, B.; Bhadbhade, M. M.; Suresh, E. *J. Chem. Soc., Dalton Trans.* **1997**, 2273.
(37) Arana, C.; Yan, S.; Keshavart-K, M.; Potts, K. T.; Abruna, H. D. *Inorg. Chem.* **1992**, *31*, 3680.
(38) Feigl, F. *Spot Tests in Organic Analysis*; Elsevier: Amsterdam, 1956; p 451.
(39) Hurrell, H. C.; Mogstad, A. L.; Usifer, D. A.; Potts, K. T.; Abruna, H. D. *Inorg. Chem.* **1989**, *28*, 1080.

(δ (ppm), DMSO-d_6): 7.70−7.92 (m, 6H), 8.22 (t, 4H), 8.54 (t, 2H), 8.66 (d, 4H), 9.00 (d, 4H), 9.20−9.34 (m, 4H). UV/vis (DMF; λ_{max}, nm (ϵ)): 380 (3.7×10^3), 294 (2.7×10^4), 280 (2.4×10^4).

[Rh(bpca)(pa)Cl][PF$_6$]·H$_2$O (3) (pa = 2-Picolinamide). Complex **1** (0.2 g, 0.36 mmol) in 1:1 ethanol−water (40 mL) was refluxed for 12 h. The light yellow solution thus obtained was concentrated to ca. 20 mL by rotary evaporation, and a saturated aqueous solution (5 mL) of NH_4PF_6 was added. The yellow precipitate which separated was isolated by filtration, washed with water, and recrystallized from acetonitrile; yield 0.19 g (81%). Anal. Calcd for $C_{18}H_{16}ClRhN_5O_4PF_6$: C, 33.28; H, 2.48; N, 10.78. Found: C, 32.96; H, 2.31; N, 10.88. Molar conductance (Λ_M, Ω^{-1} cm^2 mol^{-1}): 80. ^{1}H NMR (δ (ppm), DMSO-d_6): 7.67 (m, 4H), 8.15−8.37 (m, 7H), 8.68 (d, 2H), 9.73 (d, 1H). UV/vis (DMF; λ_{max}, nm (ϵ)): 330 (6.8×10^3), 274 (1.8×10^4).

[Rh(bpca)(tpy)][PF$_6$]$_2$·CH$_3$CN (4). Complex **1** (0.279 g, 0.5 mmol) and tpy (0.116 g, 0.5 mmol) were refluxed in 1:1 ethanol−water (40 mL) for 24 h. The volume of the solution was reduced to ca. 25 mL by rotary evaporation and filtered, and to the filtrate was added an aqueous solution (5 mL) of NH_4PF_6 (5 mmol). The pale yellow precipitate thus separated was isolated by filtration and washed with water and ethanol. Recrystallization from acetonitrile gave a pale yellow crystalline compound; yield 0.36 g (80%). Anal. Calcd for $C_{29}H_{22}RhN_7O_2P_2F_{12}$: C, 38.99; H, 2.48; N, 10.97. Found: C, 38.78; H, 2.32; N, 10.81. Molar conductance (Λ_M, Ω^{-1} cm^2 mol^{-1}): 154. ^{1}H NMR (δ (ppm), DMSO-d_6): 1.97 (s,3H), 7.58 (m, 2H), 7.66−7.75 (m, 4H), 8.21−8.41 (m, 6H), 8.55 (d, 2H), 8.90 (d, 2H), 9.00 (t, H), 9.15 (d, 2H). UV/vis (DMF; λ_{max}, nm (ϵ)): 360 (7.3×10^3), 340 (1.2×10^4), 328 (1.3×10^4), 284 (2.3×10^4).

[Rh(tpy)Cl$_3$] (5). This complex was prepared by following a procedure similar to that of complex **1**; yield 0.18 g (82%). Anal. Calcd for $C_{15}H_{11}Cl_3RhN_3$: C, 40.71; H, 2.51; N, 9.49. Found: C, 40.49; H, 2.52; N, 9.27. Molar conductance (Λ_M, Ω^{-1} cm^2 mol^{-1}): 8. ^{1}H NMR (δ (ppm), DMSO-d_6): 7.94 (m, 2H), 8.4 (t, 2H), 8.53 (t, 1H), 8.74−8.82 (m, 4H), 9.26 (d, 2H). UV/vis (DMF; λ_{max}, nm (ϵ)): 366 (2.6×10^3), 328 (2.5×10^4), 318 (2.1×10^4).

Alternative Method for the Synthesis of Complex 4. Complex **5** (0.221 g, 0.5 mmol) and tptz (0.156 g, 0.5 mmol) were refluxed in ethanol−water (2:1, 50 mL) for 24 h. The solution was then concentrated to ca. 15 mL in a rotary evaporator, and a saturated aqueous solution of NH_4PF_6 (5 mL) was added. The yellow precipitate of complex **4**, [Rh(bpca)(tpy)][PF$_6$]$_2$, was filtered off, washed with water, and recrystallized from acetonitrile; yield 0.36 g (85%). Anal. Calcd for $C_{27}H_{19}RhN_6O_2P_2F_{12}$: C, 38.05; H, 2.25; N, 9.86. Found: C, 37.92; H, 2.16; N, 9.91. Molar conductance, ^{1}H NMR and UV/vis data are similar to those for complex **4**.

[Rh(bpca)$_2$][ClO$_4$] (6). Complex **2** (0.21 g, 0.2 mmol) was refluxed in ethanol−water (1:1, 50 mL) for 36 h. The solvent was then removed by rotary evaporation, and the residue was washed with water and diethyl ether and recrystallized from boiling acetonitrile; yield 0.11 g (85%). Anal. Calcd for $C_{24}H_{16}ClRhN_6O_8$: C, 44.02; H, 2.46; N, 12.83. Found: C, 43.87; H, 2.58; N, 12.72. Molar conductance (Λ_M, Ω^{-1} cm^2 mol^{-1}): 76. ^{1}H NMR (δ (ppm), DMSO-d_6): 7.78 (m, 4H), 8.26−8.38 (m, 8H), 8.49 (d, 4H). UV/vis (DMF; λ_{max}, nm (ϵ)): 328 (1×10^4), 272 (1.8×10^4).

Caution! Perchlorate salts are potentially explosive, especially when heated.

Crystal Structure Determination of Complexes 1 and 4. A summary of crystallographic details for **1** and **4** is given in Table 1. Both structures were solved by the heavy-atom method and refined by full-matrix least-squares procedures. The non-hydrogen atoms were refined anisotropically; the H atoms located in the difference Fourier were included as in the riding model.[40] The difference map in complex **1** revealed three peaks of heights ~8, 5.4, and 1.3 e Å^{-3} which were assigned to the water molecules, one with full occupancy (O(1W)) and the other one disordered over two sites (O(2W) and O(2W′)) with occupancies of 0.75 and 0.25, respectively. In the structure of **4**, the difference map revealed a solvent (acetonitrile) molecule which has an adequate space in the channel. The atoms of the two PF_6 anions exhibit high thermal anisotropies.

Table 1. Summary of Crystallographic Data for Complexes **1** and **2**

	1	**4**
chem formula	$C_{18}H_{16}Cl_3N_6O_2Rh$	$C_{29}H_{22}F_{12}N_7O_2P_2Rh$
fw	557.63	893.34
a (Å)	11.642(2)	9.5810(10)
b (Å)	7.302(2)	12.933(2)
c (Å)	24.332(3)	14.493(2)
α (deg)	90.0(0)	82.480(10)
β (deg)	96.420(10)	71.810(10)
γ (deg)	90.0(0)	75.100(10)
Z	4	2
V (Å^3)	2055.5(7)	1646(2)
space group	monoclinic, $P2_1/c$	triclinic, $P\bar{1}$
radiation used, λ (Å)	Mo *K*α, 0.7107	Mo *K*α, 0.7107
ρ_{calcd} (g cm^{-3})	1.813	1.80
abs coeff, μ (cm^{-1})	1.251	0.721
temp (K)	295	295
final R (F_o^2)[a]	0.040	0.030
weighted R(F_o^2)[b]	0.117	0.082

[a] $R1 = \sum||F_o| - |F_c|/\sum|F_o||$. [b] $wR2 = [\sum w(F_o^2 - F_c^2)^2/\sum w(F_o^2)^2]^{1/2}$.

Programs used: CAD4 PC[41] for crystal orientation, unit cell refinement, and intensity data measurement; NRCVAX[42] for Lp correction and data reduction; SHELX-86[43] for structure solution; SHELX − 93[40] for full-matrix least-squares refinement. Graphics: ORTEP−II[44] and PLUTO.[45] Calculations of molecular geometry and intermolecular interactions: CSU.[46] All computations were performed on a Pentium-Pro PC.

Results and Discussion

Synthesis of the Complexes. The reaction of $RhCl_3·3H_2O$ with tptz (1:1 molar ratio) in ethanol resulted in the formation of [Rh(tptz)Cl$_3$]·2H$_2$O (**1**) in excellent yield. A similar reaction in ethanol−water (1:1) with longer refluxing time (30 h) was observed to promote hydrolysis of tptz to [bis(2-pyridylcarbonyl)amide] anion (bpca), yielding the complex $[Rh(bpca)_2]^+$.[36] In the present case, the absence of water, short reflux time, and precipitation of the product during reflux are the factors which could prevent the hydrolysis of tptz. However, using the same method with an appropriate ligand to metal molar ratio a bis-chelate complex, $[Rh(tptz)_2]^{3+}$, could not be prepared in pure form, as the reaction gave a mixture of complexes **1** and **2** along with a small quantity of hydrolyzed product. However, the complex [Rh(tptz)$_2$][ClO$_4$]$_3$·2H$_2$O (**2**) could be prepared using a different route involving two steps. In the first step $RhCl_3$ was treated with $AgClO_4$ in acetone under an argon atmosphere, and after removal of precipitated AgCl, tptz was added to the solution (1:2 molar ratio), which gave complex **2** in good yield. Metal-bound tptz in complexes **1** and **2** was also hydrolyzed on reflux in 1:1 ethanol−water. Thus, hydrolysis of complex **1** yielded [Rh(bpca)(pa)Cl][PF$_6$]·H$_2$O (**3**), whereas a similar reaction in the presence of 2,2′:6′,2″-terpyridine (tpy) resulted

(40) CAD-4 Software, Version 5; Enraf-Nonius: Delft, The Netherlands, 1989.
(41) Gabe, E. I.; Le Page, Y.; Charland, I. P.; Lee, F. L.; White, P. S. *J. Appl. Crystallogr.* **1989**, *22*, 384.
(42) Sheldrick, G. M. *Acta Crystallogr.* **1990**, *A46*, 467.
(43) Sheldrick, G. M. SHELX-93 Program for Refinement of Crystal Structures; University of Gottingen, Gottingen, Germany, 1993.
(44) Johnson, C. K. ORTEP II, Report ORNL-5138; Oak Ridge National Laboratory, Oak Ridge, TN, 1976.
(45) Motherwell, W. D. S.; Clegg, W. PLUTO Program for Plotting Molecular and Crystal Structures; University of Cambridge, Cambridge, England, 1978.
(46) Vickovic, I. Crystal Structure Utility (CSU), a Highly Automated Program for the Calculation of Geometrical Parameters in the Crystal Structure Analysis; Faculty of Science, University of Zagreb, Zagreb, Yugoslavia, 1988.

Scheme 1

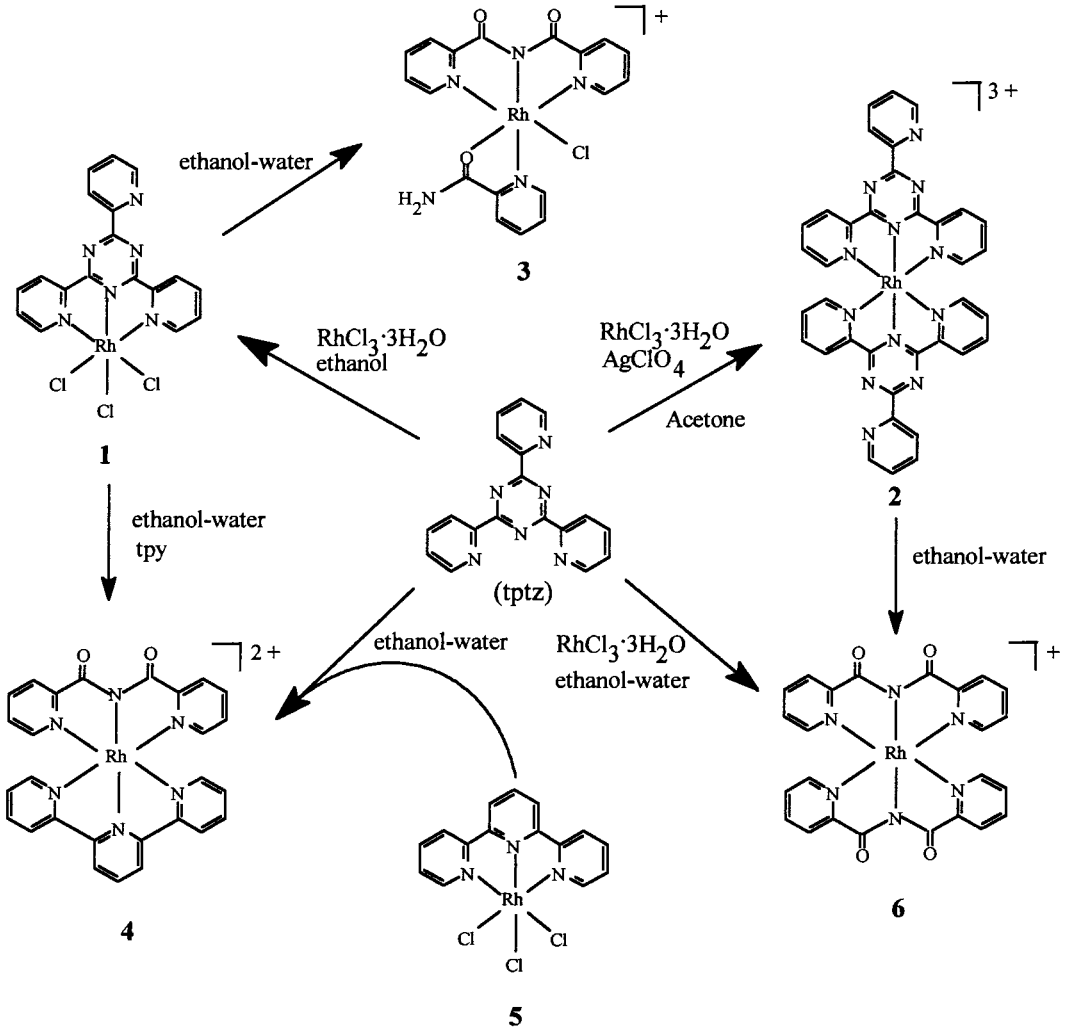

in the formation of a mixed-ligand complex, [Rh(bpca)(tpy)]-$[PF_6]_2$·CH_3CN (**4**). In complex **2**, hydrolysis of both tptz ligands occurred, yielding the complex $[Rh(bpca)_2][ClO_4]$ (**6**), similar to that synthesized earlier (only differing in the anion) by the reaction of tptz and $RhCl_3$ and characterized by a single-crystal X-ray study.[36] Only essential analytical and physicochemical data for complex **6** are given to establish the similarity. In the case of Cu(II)−tptz chemistry, it was reported that a strong tridentate ligand such as tpy when previously bound to metal ion prevents the hydrolysis of tptz, the addition of which to a water−ethanol solution of $[Cu(tpy)]^{2+}$ formed the complex $[Cu(tpy)(tptz)]^{2+}$.[35] We synthesized a terpyridine complex of Rh(III), $[Rh(tpy)Cl_3]$(**5**), by a method similar to that for complex **1**; the reaction of **5** with tptz in ethanol−water promoted the hydrolysis of tptz, giving the complex $[Rh(bpca)(tpy)][PF_6]_2$, the same as **4**. The ligand tptz and the complexes **1**−**6** are shown in Scheme 1. The molecular geometries of complexes **1** and **4** were established by single-crystal X-ray studies, discussed in a later section.

C, H, and N analyses of complexes **1**−**6** confirmed their compositions. Conductivity measurements[47] showed that complexes **1** and **5** are nonelectrolytes, indicating the chloride coordination to metal ions. Complexes **3** and **6** are 1:1 electrolytes; **2** and **4** are 1:3 and 1:2 electrolytes, respectively. As expected, PF_6^- and ClO_4^- are not coordinated to metal ions.

(47) Geary, W. J. *Coord. Chem. Rev.* **1971**, *7*, 81.

The IR spectra of complexes **3**, **4**, and **6** exhibit strong bands at 1720, 1731, and 1722 cm^{-1}, respectively, while other complexes and tptz did not show any band in that region. This band is assigned to ν(C═O) of metal-bound bpca,[32−36] formed by the hydrolysis of tptz. Complex **3** also exhibits IR bands at 3452 m, 3354 m, 3215 w, and 1662 s cm^{-1}, the first three are assigned to $-NH_2$ and the fourth one to ν(C═O) of 2-picolinamide.[34,35]

^{1}H NMR Studies. The ^{1}H NMR spectra of tptz and complexes **1**−**6** were recorded in DMSO-d_6. The spectra of tptz and complex **1** with the assignment of signals are illustrated in Figure 1. A significant downfield shift (0.35−0.62 ppm) for all protons of the metal-bound pyridyl rings is observed. The lowest field doublet (9.43 ppm, 2H) is assigned to H_6. The possibility of assigning this doublet to H_3 and merging of the H_6 doublet with the overlapping resonances centered at 9.11 ppm seems unlikely, because in that case a high deshielding of H_3 (by 0.7 ppm) and only ∼0.2 ppm downfield shift of H_6 cannot be explained, as H_6 is adjacent to the metal-bound nitrogen atoms and is expected to experience maximum deshielding effect. In the spectra of tptz and tpy, the doublets for H_3 and H_6 have characteristic J_{H-H} values of 7.8 and 5.4 Hz, respectively. The lowest field doublet in the spectrum of complex **1** shows a J_{H-H} value of 5.4 Hz, justifying the assignment of this signal to H_6. Complex **5,** where a tpy ligand is bound to metal ion in a tridentate fashion like tptz in complex

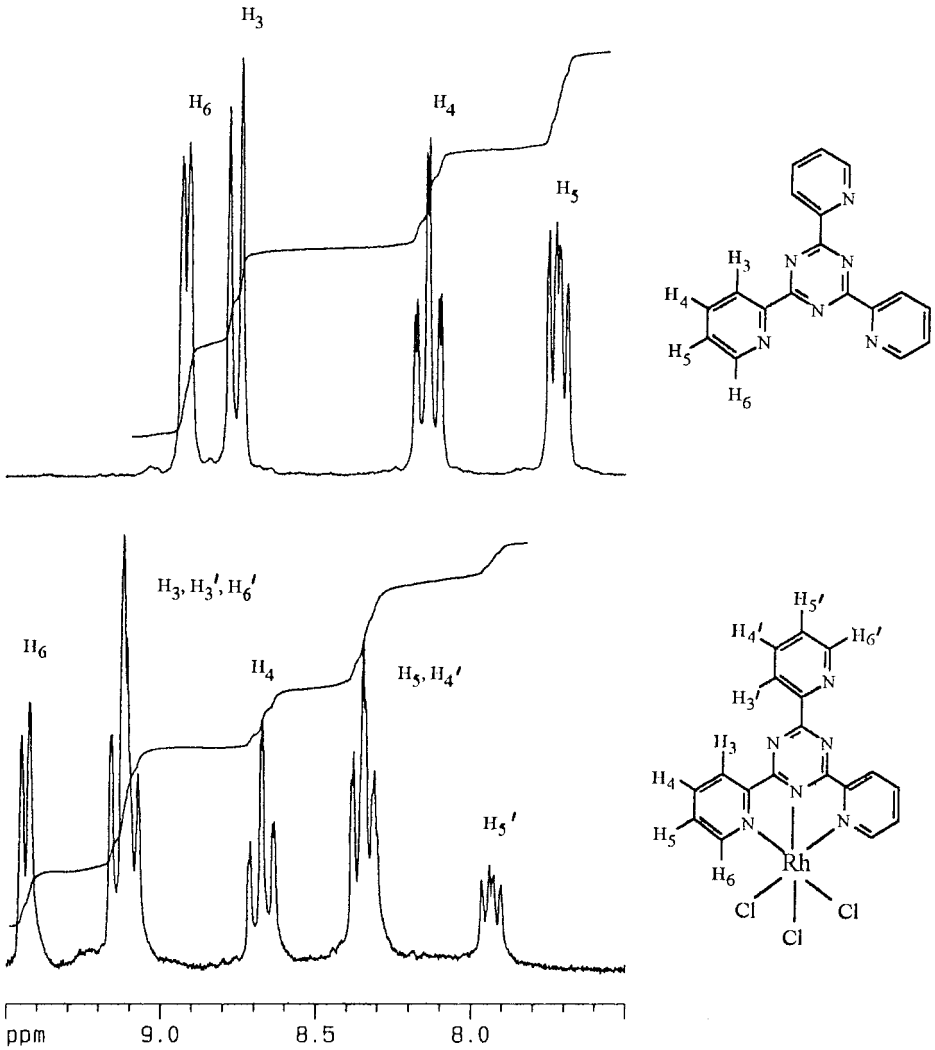

Figure 1. ^{1}H NMR spectra of tptz and complex **1** in DMSO-d_6 with assignment of protons.

1, shows a similar deshielding effect (0.2−0.55 ppm compared to free tpy) for all protons. The lowest field doublet at 9.26 ppm with $J_{H-H} = 5.4$ Hz is assigned to H_6.

Complex **2** exhibits four distinct resonances at 8.22 (triplet), 8.54 (triplet), 8.66 (doublet, $J_{H-H} = 5.4$ Hz), and 9.00 (doublet, $J_{H-H} = 7.8$ Hz), which are assigned to H_4, H_4', H_6, and H_3, respectively. The overlapping resonances in the regions 7.70−7.92 and 9.20−9.34 ppm are due to ($H_5 + H_5'$) and ($H_3' + H_6'$), respectively. Comparing these data with that of complex **1**, we note that $H_3'-H_6'$ protons have shifted slightly downfield and H_4 and H_5 have shifted slightly upfield, whereas H_6 has moved substantially upfield (by 0.77 ppm). The analogous Ru(II) complex $[Ru(tptz)_2]^{2+}$ also showed a large upfield shift for H_6, which appears at 7.75 ppm, whereas the chemical shifts of other protons are comparable to those of complex **2**.[27] A large upfield shift of H_6 can be attributed to shielding of this proton as a result of its being pointed toward the shielding face of the central pyridyl ring of the neighboring ligand.[48−50] The positions of H_6 protons with respect to the central pyridyl ring of the other ligand in $[Ru(tptz)_2]^{2+}$ [36] and **4** were measured from the X-ray structures, as illustrated in Figure 2. The distances between H_6 and the central pyridyl centroid (3.12−3.73 Å) are significantly shorter compared to that reported in some Ru(II) complexes (3.640−4.297 Å) containing a dinucleating bis-tridentate ligand and tpy.[50] However, from the angles $\angle H_6-$centroid of the pyridyl ring$-$N and $\angle H_6-N-Ru/Rh$ (shown in Figure 2) it is clear that the H_6 protons are not exactly above or below the central pyridyl ring of the neighboring ligand but are in the vicinity of the ring current zone, even then experiencing a substantial shielding effect. However, this effect alone cannot account for the striking difference in chemical shifts of H_6 in the Rh(III) complex (8.66 ppm) and in the Ru(II) analogue (7.75 ppm). The charge difference of metal ion might have contributed slightly to this, but we believe that the major contribution comes from the π-back-bonding ability of Ru(II), which increases electron density on the metal-bound nitrogen and on the adjacent atoms, introducing an additional shielding effect for H_6. The π-back-bonding effect for Rh(III) is apparently not effective. This difference between Rh(III) and isoelectronic Ru(II) has also been demonstrated by others[51,52] during NMR and kinetic studies of unsaturated small molecules coordinated to these metal centers.

The ^{1}H NMR spectrum of complex **6**, where two hydrolyzed tptz (bpca) ligands are bound to the metal ion in a symmetric

(48) Thummel, R. P.; Jahng, Y. *Inorg. Chem.* **1986**, *25*, 2527.
(49) Thummel, R. P.; Lefoulon, F.; Korp, J. D. *Inorg. Chem.* **1987**, *26*, 2370.
(50) Hanan, G. S.; Arana, C. R.; Lehn, J.-M.; Baum, G.; Fenske, D. *Chem. Eur. J.* **1996**, *2*, 1292.
(51) Foust, R. D., Jr.; Ford, P. C. *J. Am. Chem. Soc.* **1972**, *94*, 5686.
(52) Zanella, A. W.; Ford, P. C. *Inorg. Chem.* **1975**, *14*, 42.

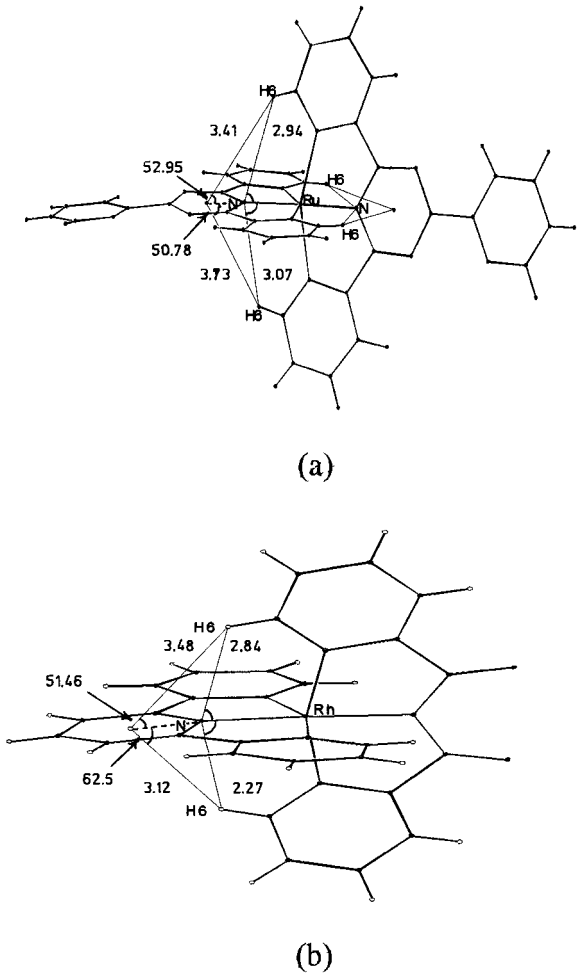

Figure 2. Stick diagrams (from X-ray data) of (a) $[Ru(tptz)_2]^{2+}$ (from ref 36) and (b) complex **4**, showing the geometry of H_6 atoms with respect to the central pyridyl centroid (distances are in Å and angles are in deg). For clarity some of the angles are shown herein: (a) $H_6-N-Ru = 77.04$ and 73.35°; (b) $H_6-N-Rh = 79.29$ and 81.64°.

fashion, exhibits resonances at 7.78 (multiplet), 8.32 (multiplet), and 8.49 ppm (doublet, $J_{H-H} = 5.6$ Hz), which are assigned to H_5, ($H_4 + H_3$), and H_6, respectively. It is interesting to note that in comparison to complex **2**, H_3 has moved substantially upfield (by 0.73 ppm), whereas H_6 lies almost at the same position as found in **2**, although H_6 should not experience a shielding effect due to the ring current of the neighboring ligand, as the bpca moiety has no central pyridyl ring and the terminal rings are far away from H_6. A significant upfield shift of both protons (H_3 and H_6) can be explained by considering the fact that the negative charge on the central nitrogen atom of the bpca moiety increases the electron density on neighboring atoms, and this effect resulted in shielding of H_3 and H_6. Complexes **3** and **4** also contain the bpca moiety, but due to the presence of secondary ligands having pyridyl units and overlapping of resonances at some important regions, it is difficult to assign peaks for the protons of primary interest. However, in complex **4,** it is expected that the H_6 of bpca should experience a shielding effect due to ring current from the central ring of the neighboring tpy but a similar effect for the H_6 of tpy seems unlikely because there is no central ring in bpca.

Electronic Spectra. The UV−vis spectra of complexes **1**−**6** were recorded in DMF, and the data are presented in the Experimental Section. The low-energy bands at 400, 380, and 366 nm of complexes **1**, **2**, and **5** are assigned to metal-to-ligand charge transfer (MLCT) transitions.[53,54] In complex **3,** the low-energy band at 330 nm may be of MLCT character but the possibility of σ-bond-to-ligand charge transfer (SBLCT) cannot be ruled out.[55,56] The mixed-ligand complex **4** exhibits two bands at 360 and 340 nm; a comparison of these bands with those of complexes **5** and **3** suggests that the 360 nm band is due to a Rh→tpy MLCT transition and the 340 nm band has MLCT or SBLCT character associated with the bpca moiety. The high-energy bands of all complexes are ligand-centered (LC) due to $\pi-\pi^*$ transition.[29,30]

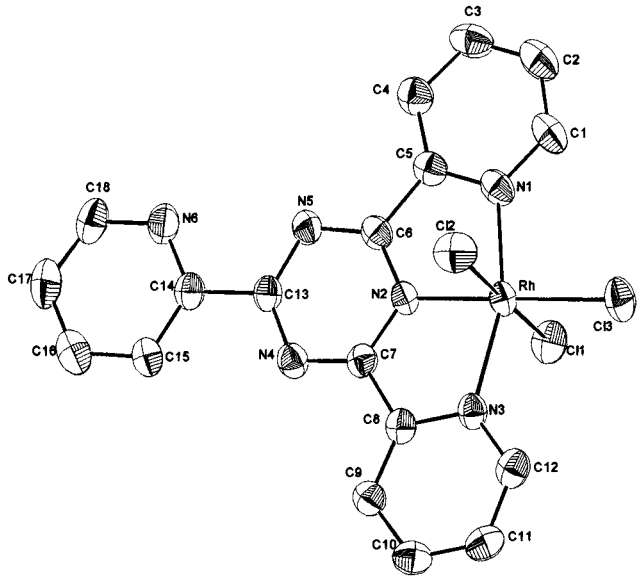

Figure 3. ORTEP view (50% probability) with atom-labeling scheme of complex **1**. Hydrogen atoms are omitted for clarity.

Crystal Structure. Complex 1. A perspective view (ORTEP)[44] of the complex with the atom numbering is shown in Figure 3; selected bond distances and angles are given in Table 2. The molecular geometry of **1** is of considerable interest, as this is the first example of intact tptz bound to the metal ion, known to promote the hydrolysis. The tptz acts as a tridentate ligand: one nitrogen from the triazine and two from pyridyl moieties along with three chlorides form the distorted-octahedral geometry around Rh(III). Three nitrogen atoms from the ligand and Cl(3) form the equatorial base, and two chlorides, Cl(1) and Cl(2), are in axial positions. The least-squares plane through the atoms N(1), N(2), N(3), and Cl(3) has a slight tetrahedral bias (average deviations ±0.04 Å) and the Rh ion is contained well within this range. The source of distortion primarily comes from the bites taken by the ligand, the bite angles N(1)−Rh−N(2) and N(2)−Rh−N(3) being 79.4(2) and 80.25(15)°, respectively, significantly smaller than the ideal value of 90° because of the constraint imposed by the five-membered chelate rings. The bond distance of Rh to the middle nitrogen N(2) (1.924(4) Å) is significantly shorter (by about 0.12 Å) than the Rh−N(1) (2.045(4) Å) and Rh−N(3) (2.060-(4) Å) distances, a pattern observed in this type of three-point attachment of tptz-like ligands. The Rh−Cl distances vary from 2.3293(13) to 2.3504(13) Å; the longest distance of Rh−Cl(1) could be due to strong H-bonding interaction with the water

(53) Juris, A.; Balzani, V.; Barigelletti, F.; Campagna, S.; Belser, P.; Zelewsky, A. V. *Coord. Chem. Rev.* **1988**, *84*, 85.
(54) MacQueen, D. B.; Petersen, J. D. *Inorg. Chem.* **1990**, *29*, 2313.
(55) Didier, P.; Ortmans, I.; Krisch-DeMesmaelker, A.; Watts, R. J. *Inorg. Chem.* **1993**, *32*, 5239.
(56) Ortmans, I.; Didier, P.; Krisch-DeMesmaelker, A. *Inorg. Chem.* **1995**, *34*, 3695.

Table 2. Selected Bond Lengths (Å) and Angles (deg) for Complexes **1** and **4**

	Complex **1**		
Rh−N(1)	2.045(4)	Rh−Cl(1)	2.350(1)
Rh−N(2)	1.924(4)	Rh−Cl(2)	2.329(1)
Rh−N(3)	2.060(4)	Rh−Cl(3)	2.346(1)
N(1)−Rh−N(2)	79.4(2)	Cl(1)−Rh−Cl(2)	178.16(5)
N(2)−Rh−N(3)	80.25(15)	N(2)−C(6)−C(5)	112.8(4)
N(3)−Rh−Cl(3)	98.80(10)	N(2)−C(7)−C(8)	113.4(4)
N(1)−Rh−Cl(3)	101.58(11)	N(2)−C(7)−N(4)	121.5(4)
N(1)−Rh−N(3)	159.61(15)	N(2)−C(6)−N(5)	122.1(4)
N(2)−Rh−Cl(3)	176.74(11)		
	Complex **4**		
Rh−N(1)	2.044(2)	Rh−N(5)	1.971(2)
Rh−N(2)	2.004(2)	Rh−N(6)	2.057(2)
Rh−N(3)	2.038(2)	C(6)−O(1)	1.207(3)
Rh−N(4)	2.045(2)	C(7)−O(2)	1.206(3)
N(1)−Rh−N(2)	81.37(9)	N(2)−C(7)−C(8)	110.7(2)
N(2)−Rh−N(3)	81.25(9)	N(2)−C(6)−O(1)	128.1(3)
N(3)−Rh−N(5)	99.98(9)	N(2)−C(7)−O(2)	127.7(3)
N(1)−Rh−N(5)	97.40(9)	N(5)−C(18)−C(17)	112.8(2)
N(1)−Rh−N(3)	162.62(9)	N(5)−C(22)−C(23)	113.0(2)
N(2)−Rh−N(5)	178.24(8)	N(5)−C(18)−C(19)	118.9(3)
N(4)−Rh−N(6)	160.36(9)	N(5)−C(22)−C(21)	119.6(3)
N(2)−C(6)−C(5)	110.9(2)		

molecule O(1W). In the ligand, the $C(sp^2)-C(sp^2)$ distances within the ring are normal (average 1.379(7) Å) and the exterior bonds C(5)−C(6), C(7)−C(8), and C(13)−C(14) average to 1.473(6) Å. The tptz shows a considerable overall planarity; the three pyridyl rings are twisted with respect to the central triazine ring by a maximum of ∼3.3°. Interestingly, analysis of intermolecular contacts reveals the close approach of O(1W) and the major site of O(2W) toward the atoms C(6) and C(7), respectively (O(1W)···C(6) = 3.024(6) Å and O(2W)···C(7) = 3.058(8) Å), the carbon atoms at which nucleophilic attack takes place. These short contacts provide an insight into the mechanism of hydrolysis (discussed later). The water molecule O(2W) is linked through one of its hydrogens to O(1W), which in turn makes an H-bond with Cl(1). The structure contains several C−H···O interactions[57] and one O(1W)-H(2W1)···N(6) short contact.

Complex 4. A perspective view (ORTEP)[44] of **4** is shown in Figure 4 along with the labeling of atoms. Selected bond distances and angles are given in Table 2. Two tridentate ligands, the bpca moiety and tpy, are coordinated to the metal ion through their N atoms in a mutually perpendicular fashion, which provides a distorted-octahedral geometry at rhodium. The source of distortion, as in **1**, is because of the formation of five-membered chelate rings; the bites, N−Rh−N, taken by the terpyridyl ligand are slightly smaller (average 80.18(9)°) than those taken by the bpca (average 81.31(9)°). The nitrogen atoms of bpca, N(1), N(2), and N(3), and the nitrogen of the middle ring of tpy, N(5), show a slightly higher degree of planarity compared to the plane through the nitrogens of tpy, N(4), N(5), and N(6), and N(2) of bpca, although the Rh atom is contained well within the plane in either case. In both of the ligands, Rh to central N atom distances are shorter than the other two wing Rh−N distances (Table 2). In the case of the bpca moiety, the average of Rh−N(1) and Rh−N(3) (2.041(2) Å) distances differs from Rh−N(2) (2.004(2) Å) by 0.037 Å, whereas in case of terpyridyl this difference is significantly higher (0.08 Å). The bpca moiety is more planar (except for O(1), which deviated by 0.138(5) Å) than the tpy; the angle between the two pyridyl

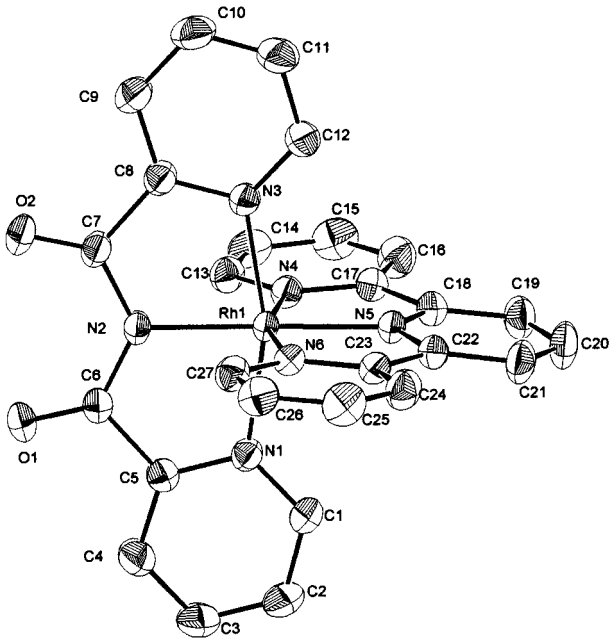

Figure 4. ORTEP view (50% probability) with atom-labeling scheme of complex **4**. Hydrogen atoms are omitted for clarity.

Chart 1

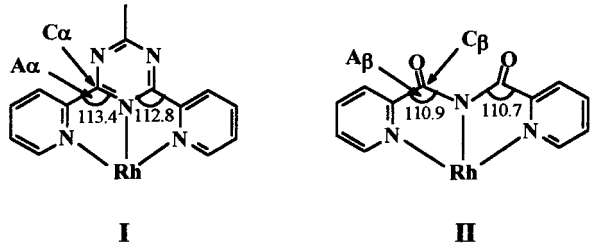

I **II**

rings in the former is only 3.1(2)°, whereas in the latter the two wing pyridyl rings are rotated with respect to the middle ring by 4.64(2) and 8.03(2)°, respectively. The two PF_6 anions show very high thermal anisotropies, and so do the atoms of the acetonitrile. The packing of the molecules shows a channel occupied by the acetonitrile. There are several C−H···O and C−H···F short contacts in the crystal lattice that can be considered as meaningful interactions.[57]

Mechanistic Aspects of the Hydrolytic Reaction. The mechanism of metal-induced hydrolysis of tptz has been of considerable interest. The crystal structure data of the copper(II) complexes of hydrolyzed tptz showed that the angles at the carbonyl carbon atoms within the chelate ring, A_β (structure II of Chart 1), are in the range 110−111.7°,[32−35] which are compressed significantly from the ideal value of 120°, rather close to the value expected for the "tetrahedral intermediate" of the hydrolysis by nucleophilic attack. On the basis of these data it was suggested that the metal-induced angular strain at C_α (structure I of Chart 1) causes the hydrolysis of the ligand.[33,35] However, recently we reported crystal structures of complex **6** (with PF_6^- counteranion) and the Ru(II) analogue of complex **2**,[36] where the average value of A_β in the rhodium complex (111.6°) is comparable to the value of A_α in the ruthenium complex (112.5°), indicating similar angular strain at C_α/C_β. The structure of complex **1** is interesting, as it provides an opportunity to study the "strain-factor" in a complex where intact tptz bound to rhodium(III) undergoes hydrolysis. It is noteworthy that the average value of A_α in **1** (113.1(4)°) is similar to that of the Ru(II) complex (112.5°), but hydrolysis

(57) Desiraju, G. R. *Acc. Chem. Res.* **1991**, *24*, 290; *Angew. Chem., Int. Ed. Engl.* **1995**, *34*, 2311.

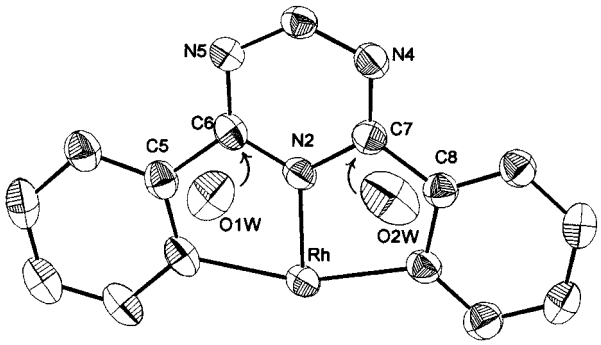

Figure 5. Partial view (ORTEP) of complex **1**, showing the interactions between water molecules and electrophilic carbon atoms.

of tptz occurred only in the case of the rhodium complex and not in the ruthenium complex under similar experimental conditions. These observations, therefore, suggest that the metal ions play a major role in the hydrolytic process. After coordination of tptz to the metal ion, the ligand to metal σ-donation (L → M) results in an enhanced electrophilicity on the carbon atoms ($C^{\delta+}$) adjacent to the metal-bound nitrogen atom of the triazine ring, thus making it (C_β) susceptible to the nucleophilic attack. The short contacts observed between water and carbon atoms of triazine in **1** are significant in this context.

A partial (ORTEP) view of complex **1** (Figure 5) shows O(1W) and O(2W) approaching toward the carbon atoms C(6) and C(7), respectively, which are to be hydrolyzed. The C(6)···O(1W) and C(7)···O(2W) distances of 3.024(6) and 3.058(8) Å, respectively, indicate significant interactions between water molecules and the electrophilic carbon centers created by the electron-withdrawing effect of the metal ion. This molecule, therefore, may be considered as a model close to the "intermediate" of hydrolysis by nucleophilic attack. This type of "intermediate" generally shows tetrahedral geometry; however, in this case C(6) and its associated atoms N(2), N(5), and C(5) form an excellent plane. The deviation of C(6) from the plane defined by other three atoms is only 0.008 Å and the summation of three angles around C(6) is 360°; the oxygen atom O(1W) approaches toward C(6) along a direction perpendicular to this plane (∠O(1W)−C(6)−N(5) is 89.9(3)°), suggesting a trigonal-pyramidal geometry for the intermediate. Atom C(7) also shows similar geometry with O(2W) at the apical position. Even with a closer contact of water and carbon atoms (a true "intermediate") it is difficult to pull out C(6)/C(7) significantly from the basal plane, as they are the constituents of a six- as well as a five-membered ring having excellent planarity. In the case of the ruthenium(II) complex, the metal ion has the ability to form π-back-bonding with unsaturated ligands compensating partially for the σ-electron-withdrawing effect. As a result, the electron density on the carbon atoms of the triazine ring in the ruthenium(II) complex increases compared to that in its rhodium(III) analogue; the π-back-bonding in the latter case is apparently not effective. Therefore, it is difficult to create an electrophilic carbon atom in the triazine ring bound to ruthenium(II). The water molecule in $[Ru(tptz)_2][PF_6]\cdot H_2O$[36] is located at a site similar to that found in complex **1**, making H-bonding with the CH of the same pyridyl ring as occurs in **1** (C(4)−H(4) and O(1W)), but the distance C(6)···O(1W) of 3.908 Å does not indicate any significant interaction. This observation suggests that the carbon atoms of the triazine ring in the Ru(II) complex are not sufficiently electropositive to interact with the water oxygen. Kinetics and NMR studies of rhodium(III) and analogous ruthenium(II) complexes[51,52] are in agreement with these characteristics of the metal ions. There are also other examples of copper(II) and nickel(II) complexes which have activated ligands making electron-deficient carbon atoms susceptible to the nucleophilic attack.[58−61] We, therefore, suggest that a decrease in π-electron density at the carbon atoms of the triazine ring by an electron-withdrawing effect of the metal ion is the predominant factor, rather than angular strain, in the metal-promoted hydrolysis of tptz. Currently we are investigating the reactions of tptz with other metal ions.

Electrochemistry. Cyclic voltammograms of all complexes were recorded in DMF, and the data are presented in Table 3. All Rh(III) complexes showed initially a large irreversible reduction wave at negative potential followed by one or two quasi-reversible redox couples. In analogy to the reported electrochemical data of Rh(III)−polypyridyl complexes,[62−65] it appears that the first large cathodic peak is metal-centered and it is in fact a composite wave corresponding to 2e reduction (Rh(III) → Rh(I)); the other redox couples at more negative potentials are ligand-based 1e process. The resolution of the composite wave into two components at higher scan rate (>10 V/s) as found for some complexes[62,63] could not be observed when the scan rate was increased up to 10 V/s. When the potential scan is reversed just after the first reduction wave, no anodic peak was observed except for **4**, which showed a small anodic current. These observations indicate that chemical changes occurred in the complexes during the metal reduction.

Cyclic voltammograms of solutions saturated in CO_2 were also recorded for all the complexes. Figure 6 shows the cyclic voltammograms of complexes **1**, **4**, and **5** under argon and carbon dioxide atmospheres. The current enhancement in CO_2-saturated solutions relative to those under argon are indicative of the electrocatalyzed reduction of CO_2.[37,64−69] It is interesting to note that addition of trace water to the solution increased current enhancement, which was maximum (about 30% increased compared to that found in dry solvent) when ∼0.2 mL of water was added to 10 mL of solution. However, addition of more water did not enhance the current significantly. This observation indicates that the presence of proton donors influences the electrocatalytic reduction of CO_2. It may be noted that the metal reduction waves (2e) in the voltammograms of complexes **2**−**5** under carbon dioxide were split, which can be attributed to the interaction of CO_2 with the metal ion at the early stage of metal reduction. To our knowledge, the splitting of a metal reduction peak for Rh(III)−polypyridyl complexes under CO_2 has not been reported so far; it was observed under a nitrogen atmosphere with a high scan rate (>30 V/s).[62,63] However, some Fe(II)− and Ni(II)−polypyridyl complexes under a carbon dioxide atmosphere showed a new wave, close to the metal reduction peak, due to partial displacement of the ligand and coordination by solvent (CH_3CN).[37] Table 3 lists

(58) Komiya, S.; Suzuki, S.; Watanabe, K. *Bull. Chem. Soc. Jpn.* **1971**, *44*, 1440.
(59) Storhoff, G. N.; Lewis, H. C., Jr. *Coord. Chem. Rev.* **1977**, *23*, 1.
(60) Michelin, R. A.; Mozzon, M.; Bertani, R. *Coord. Chem. Rev.* **1996**, *147*, 299.
(61) Paul, P.; Nag, K. *Inorg. Chem.* **1987**, *26*, 1586.
(62) Kew, G.; De Armond, K.; Hanck, K. *J. Phys. Chem.* **1974**, *78*, 727.
(63) Kew, G.; Hanek, K.; De Armond, K. *J. Phys. Chem.* **1975**, *79*, 1828.
(64) Bolinger, C. M.; Story, N.; Sullivan, B. P.; Meyer, T. J. *Inorg. Chem.* **1988**, *27*, 4582.
(65) Rasmussen, S. C.; Richter, M. M.; Yi, E.; Place, H.; Brewer, K. J. *Inorg. Chem.* **1990**, *29*, 3926.
(66) Collin, J. P.; Sauvage, J. P. *Coord. Chem. Rev.* **1989**, *93*, 245.
(67) Bolinger, C. M.; Sullivan, B. P.; Conrad, D.; Gilbert, J. A.; Story, N.; Meyer, T. J. *J. Chem. Soc., Chem. Commun.* **1985**, 796.
(68) Cheng, S. C.; Blaine, C. A.; Hill, M. G.; Mann, K. R. *Inorg. Chem.* **1996**, *35*, 7704.
(69) Ali, M. Md.; Sato, H.; Mizukawa, T.; Tsuge, K.; Haga, M.; Tanaka, K. *J. Chem. Soc., Chem. Commun.* **1998**, 249.

Table 3. Cyclic Voltammetric Data for Rhodium(III) Complexes

complex	under argon atmosphere				under CO_2 atmosphere
	$E_{p,a}$, V	$E_{p,c}$, V	$E_{1/2}$, V	ΔE_p (mV)	$E_{p,c}(CO_2)$,[b] V
$[Rh(tptz)Cl_3]\cdot 2H_2O$ (**1**)		−0.42			−1.28
	−0.86	−0.93	−0.89	70	
$[Rh(tptz)_2][ClO_4]_3\cdot 2H_2O$ (**2**)		−0.78			−1.36
	−1.04	−1.13	−1.08	90	
	−1.43	−1.60	−1.51	170	
$[Rh(bpca)(pa)Cl][PF_6]\cdot H_2O$ (**3**)		−0.98			−1.26
	−1.45	−1.53	−1.49	80	
$[Rh(bpca)(tpy)][PF_6]_2\cdot CH_3CN$ (**4**)		−0.76			−1.44
	−1.46	−1.53	−1.50	70	
	−1.76	−1.85	−1.80	90	
$[Rh(tpy)Cl_3]$ (**5**)		−0.65			−1.40
	−1.30	−1.37	−1.34	70	

[a] Potential of the anodic peaks. [b] Potential of the wave at which reduction of carbon dioxide was observed. [c] Potential of the cathodic peaks.

Table 4. Electrocatalytic Data for the Reduction of Carbon Dioxide

complex	applied potential[a]	charge passed,[b] C	HCO_2^- charge,[c] (efficiency, %)	turnovers[d]
$[Rh(tptz)Cl_3]\cdot 2H_2O$ (**1**)	−1.33	348.6	280.2 (81.5)	10.8
$[Rh(tptz)_2][ClO_4]_3\cdot 2H_2O$ (**2**)	−1.41	434.8	305.7 (71.1)	9.1
$[Rh(bpca)(pa)Cl][PF_6]\cdot H_2O$ (**3**)	−1.31	263.2	176.8 (68.4)	7.6
$[Rh(bpca)(tpy)][PF_6]_2\cdot CH_3CN$ (**4**)	−1.49	442.0	342.7 (78.4)	9.5
$[Rh(tpy)Cl_3]$ (**5**)	−1.45	235.5	191.0 (82.8)	6.8

[a] Potential at which electrocatalytic experiments were carried out. [b] Total charge passed by the electrode; electrolyses were carried out for 5−6 h. [c] Amount of charge consumed for formate formation. [d] Turnovers for the production of formate only; turnover numbers were calculated from moles of formate produced per mole of catalyst per hour.

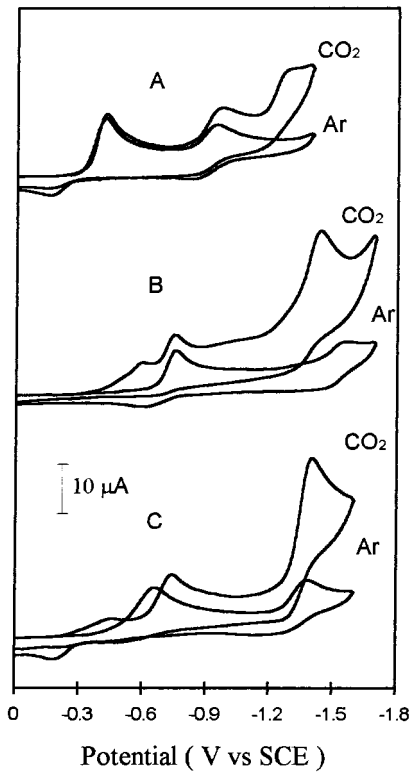

Figure 6. Cyclic voltammograms of 1.0 mM solutions of complexes **1** (A), **4** (B), and **5** (C) recorded under argon and carbon dioxide atmospheres in *dry* DMF with a scan rate of 100 mV/s. All three pairs of voltammograms have same scale of *x* and *y* axes.

the potential of the peak at which electrocatalytic reduction of CO_2 was observed; the data (−1.26 to −1.44 V) indicate a strong elecrocatalytic effect since the reduction of CO_2 in DMF in the absence of catalyst occurred at a potential more negative than −2.0 V.[37]

Controlled-potential carbon dioxide reduction catalysis experiments were performed in a three-compartment cell by using Pt gauze as the working electrode and tetrabutylammonium tetrafluoroborate as the supporting electrolyte in DMF containing 2.5% water saturated with CO_2. The electrolysis experiments were conducted for 5−6 h; the current dropped slightly during the first few minutes and remained fairly constant (±20%) throughout the remainder of the experiments. After the catalytic run, the amount of formic acid produced in the reaction mixture was estimated by a chromotropic acid test. Since the production of HCO_2^- requires 2e, the amount of current consumed in formate formation and also the current efficiency could be calculated. The protons required for the production of formic acid can be obtained from added water and supporting electrolyte.[37,64−67] Meyer et al.[64] showed that in the absence of H_2O the protons required for the reduction products were derived from the tetra-*n*-butylammonium ion (supporting electrolyte); the amount of NBu_3 thus produced was also determined. However, in the presence of water no NBu_3 but rather formate was produced, indicating that H_2O acted as the proton source.[64] Our experiments show that addition of H_2O up to ∼2.5% increased current consumption as well as production of formate; although addition of more water slightly increased the current consumption, it decreased the current efficiency for formate formation. The electrocatalytic data are presented in Table 4. The current efficiency and turnovers exhibited by these new complexes are quite similar to those reported for bis-chelate Rh(III) complexes of bipyridyl[64,67] and bridging polypyridyl ligands[65] but higher than those for Ir(III)−polypyridyl complexes.[65] The possibility of the formation of oxalate as a reduction product was ruled out on the basis of ^{13}C NMR spectral analysis (see Experimental Section). Oxalate formation generally takes place under aprotic conditions,[69−71] but in the

(70) Kushi, Y.; Nagao, H.; Nishioka, T.; Isobe, K.; Tanaka, K. *Chem. Lett.* **1994**, 2175.
(71) Tanaka, K.; Kushi, Y.; Tsuge, K.; Toyohara, K.; Nishioka, T.; Isobe, K. *Inorg. Chem.* **1998**, *37*, 120.

presence of proton donors (H_2O, Bu_4NBF_4) the same complexes produced formate as a major product.[69,70] Rh(III)−polypyridyl complexes, in particular, produced mainly formate;[64,65,67] however, in few cases H_2 was also reported as a minor product.[64,67] In our systems, since slow purging of CO_2 was continued during electrolysis to maintain the analytical solution saturated in CO_2,[39] analysis of gaseous products was not carried out.

Conclusions. Simple synthetic methods have been developed by which Rh(III) complexes of intact and hydrolyzed tptz (bpca) can be prepared in excellent yield. The metal-promoted hydrolysis of tptz is interesting, because this reaction results in the formation of a class of compounds containing bis(aryl)-carboximidato ligand, which is otherwise difficult to synthesize. The new complexes contain remote uncoordinated bidentate donor set(s) (N/O) on one or both sides of the metal ion, which can be used as building blocks to develop supramolecular metal complexes. The geometrical parameters of **1**, **4**, and other complexes reported recently by us clearly established that the electron-withdrawing effect of the metal ion is a predominant factor, rather than the angular strain, responsible for the metal-promoted hydrolysis of tptz. The trigonal-pyramidal geometry of the electrophilic carbon atoms ($C^{\delta+}$) of the triazine ring in complex **1** indicate that in this case the "tetrahedral intermediate", usually found in hydrolysis by nucleophilic attack, seems unlikely. The most important finding is that the new complexes show effective catalytic properties in the electrocatalytic reduction of carbon dioxide.

Acknowledgment. We are grateful to the Department of Science and Technology (DST), Government of India, for financial support. Our sincere thanks to Dr. S. D. Gomkale, Director of this institute, Dr. R. V. Jasra, and Professor P. Natarajan for their keen interest, encouragement and valuable suggestions in this work. We are grateful to the reviewers for their observations and valuable suggestions regarding NMR and electrochemical studies. We also thank Mr. P. S. Subramanian and Mr. V. Boricha for recording NMR and IR spectra.

Supporting Information Available: Two X-ray crystallographic files, in CIF format, for the structure determinations of complexes **1** and **4** are available. A table of hydrogen bonding parameters for **1** and **4** (1 page). Access and ordering information is given on any current masthead page.

IC9709739